Micro-structural, Morphological and Optical Properties of Pure and Metal (Mn & Mg) Doped ZnO Thin Films by Low Cost SILAR Method

K. Radhi Devi[1], G. Selvan[2], M. Karunakaran[3,*] and K. Kasirajan[3]

[1]Department of Physics, Sethupathy Government Arts College, Ramanathapuram-623502, India
[2]Department of Physics, Thanthai Hans Roever College, Perambalur-621220, India
[3]Department of Physics, Thin Films and Nanoscience Lab, Alagappa Government Arts College, Karaikudi-630003, India

*Corresponding author: E-mail: tvdkaruna@gmail.com

Pure and metals (Mn & Mg) doped zinc oxide (ZnO, ZnO/Mn and ZnO/Mg) thin films have been successfully grown onto a glass substrates by low cost SILAR method. The structural, morphological, compositional, functional group and optical properties of the prepared films were studied using X-ray diffraction, scanning electron microscope and EDAX, FTIR and UV-visible spectrophotometer, respectively. The structure of the films were found to be hexagonal with polycrystalline in nature with preferential orientation along (002) plane. From Fourier Transform Infrared spectroscopy, the presence of functional groups and its corresponding molecular vibrations were assessed. In UV-visible spectroscopy, the obtained direct optical band gap values 3.46, 3.56 and 3.7 eV for pure, Mn and Mg doped ZnO thin films, respectively. Morphological results showed that the remarkable changes in morphology due to the effect of metal doping. EDAX studies showed that the presence of zinc and oxygen content and also a doping metal ions.

Keywords: Doped zinc oxide, Thin Films, Morphological Studies, Compositional analysis.

INTRODUCTION

The development of novel spintronic materials and spin-based electronic devices is a hot topic of current research in materials science and condensed matter physics. Dilute magnetic semiconducting nanomaterials have received much attention because of their combined properties and multiple potential applications. Diluted magnetic oxide (DMO) research is a growing field of interdisciplinary study like spintronic such as biomedical, magnetic resonance imaging and telecommunication devices. The research going on ZnO semiconductor because outstanding physico-chemical properties and have the three forms such as zinc blende, rock salt and wurtzite. Because of hexagonal wurtzite phase of ZnO is more stable at room temperature [1-4]. Zinc oxide, a large excition binding energy of 60 meV, a wide band gap (3.37 eV) has been extensively studied due to its intrinsic properties and has attracted much attention for possible applications in optoelectronic devices such as field-effect transistors, resonators, gas sensors and solar cells, and as a catalyst [5-7]. Another promising property of

zinc oxide is low toxicity, abundance in nature, good electrical properties, large piezoelectric constants, strong luminescence and strong sensitivity of surface conductivity [8].

The doping is important key factor for change the property of a material. Zinc oxide is one of transparent conducting oxide (TCO) materials as well as one of II-VI semiconductor materials. Many materials were doped to ZnO to change optical and electrical properties. The doping of a selective element into ZnO is the primary method for controlling the properties such as band gap or electrical conductivity, and to increase the carrier concentration for electronic applications where higher carrier concentration is required. Recently, many studies have focused on the doping of transition metals such as Mn, Ni, Fe, Co and Cr into ZnO due to the potential applications in spintronic [9-12].

The magnesium oxide is a wide band gap material, ZnO:Mg is a semiconductor composed of two materials, zinc oxide and magnesium oxide, which can be easily controlled over a wide range of temperatures because the ionic radii are similar to Mg^{2+} ionic radius (0.57 Å), which has comparable ionic radius

to Zn^{2+} ion (0.60 Å) which makes Mg as suitable dopant can replace Zn atom in the lattice [13]. Rouchdi *et al.* [14] have studied the characteristics of Mg doped ZnO thin films and showed that Mg/ZnO thin films has hexagonal wurtzite structure, and grain size and band gap are increased by increasing Mg concentration. The minimum electrical resistivity of 3.45 × 10^{-2} (Ω.cm) was obtained for ZnO:Mg thin film (2 at. %).

Transition metals are used as doping chemical elements into a specially semiconductor host matrix. Mn-doped III-V semiconductors were found to be the transition metal ions (*e.g.* Mn^{2+}, Fe^{2+}, Co^{2+} and Ni^{2+}) could introduce ferromagnetic character while its semi-conducting property is retained. Through different transition metal doping ZnO, Mn has the advantage, because of its high moment, relatively small ionic radii difference between Mn^{2+} and Zn^{2+} [15,16]. Yang and Zhang [17] have studied the structural, optical and magnetic properties of Mn-doped ZnO thin films prepared by sol-gel method and showed that Mn doping does not change the wurtzite structure of ZnO. The small (0 0 2) peak broadening the increase of the Mn content, which indicates the crystal quality decreases with an increase of Mn content. The saturation magnetization Mn increased to 3.523 μ$_B$/Mn for x = 0.05, and then decreased to 1.764 μ$_B$/Mn for x = 0.07 [17].

The Mn/Mg doped ZnO thin films were prepared by different methods such as spray pyrolysis method, sol-gel, pulsed laser deposition, chemical bath deposition and SILAR method [18-22]. Among these methods, SILAR attracts more interests because it offers several advantages such as high chemical homogeneity, low processing temperature, possibility of controlling the size and morphology of particles, simplicity and low cost.

In this study, we have prepared (Mn, Mg) doped ZnO thin films through SILAR route and characterized them thoroughly by several techniques. The influence of different Mn and Mg doping on structural, optical and morphological studies has been investigated in the present work.

EXPERIMENTAL

SILAR method: Successive ionic layer adsorption and reaction (SILAR) is one of the chemical method which is used to prepare the films on any substrate. The preparation of the films using SILAR method has four steps: (a) adsorption: cations present in the precursor solution are adsorbed on the surface of the substrate, (b) first rinsing: loosely adsorbed ions are removed, (c) reaction: anions in the anionic solution forms the films on the substrate due to the reaction between cations and anion; and (d) second rinsing: all the unreacted and loosely bound ions are removed from the substrate.

Preparation of the films: Before deposition cleaning the substrate is the most important step for deposition of the films. Dust and fingerprints are the comely expected contaminants which affect the formation of the films in terms of stability, purity and morphology. The expected contaminants are set free from the substrate while cleaning. In this work, glass is chosen as the substrate. The glass substrate is cleaned by chromic acid followed by cleaned with acetone several times. The well cleaned substrates are immersed in the solution which comprising 0.1 M zinc sulphate, 0.2 M sodium hydroxide at 90 °C. This forms sodium zincate bath and the pH value of sodium zincate solution is 9. After the immersion of substrate in sodium zincate bath for 10 s, it is immersed in hot water for 10 s. This process is repeated for 100 times to prepare undoped ZnO films. The ZnO films on the substrate is formed according to the following equations:

$$ZnSO_4 + 2NaOH \longrightarrow Na_2ZnO_2 + H_2SO_4$$

$$Na_2ZnO_2 + H_2O \longrightarrow ZnO + 2NaOH$$

To prepare Mn or Mg doped ZnO films, the addition of MnSO$_4$ or MgSO$_4$, respectively, sodium zincate bath in the ratio of Zn:Mn or Zn:Mg as 100:1 leads to the formation of Mn doped ZnO films or Mg doped ZnO films. All the prepared films are dried and then annealed at 300 °C for about 2 h.

RESULTS AND DISCUSSION

Thickness measurement: In this work, thickness of the samples was measured using weight gain method. The well-cleaned glass plate is weighted in a high precision microbalance. After deposition the coated glass plate is weighted. The difference in weight gives the mass of deposited film "m". The area over the film deposition is measured as "A". The standard value of density "ρ" has been taken and the thickness (t) is calculated using the following expression:

$$t = m/(A\rho) \text{ (microns)} \qquad (1)$$

The calculated thickness values are presented in Table-1.

TABLE-1
MICRO-STRUCTURAL PROPERTIES
(Mn & Mg) DOPED ZnO THIN FILMS

Micro-structural parameters	Pure ZnO	Mn doped ZnO	Mg doped ZnO
Thickness (nm)	410	424	435
Crystallite size (nm)	43.77	37.80	32.49
Dislocation density × 10^{14} (lines/m)	5.218	6.995	9.470
Strain × (10^{-3} lines^{-2} m^{-4})	1.186	1.375	1.596
No. of crystalline per unit area (N$_C$) × 10^{15}	4.880	7.844	1.267
Lattice distortion × 10^{-3}	2.675	3.093	3.596

XRD analysis: The structural identification of the prepared ZnO thin film is confirmed by X-ray diffraction techniques as shown in Fig. 1(a). In XRD pattern, the peaks (100), (002), (101), (102) and (110) were located at 31°, 34°, 36°, 47°, 56° and 62°, planes clearly indicates the formation of ZnO thin films. The absence of secondary peaks is the clear evidence that prepared samples are pure with impurities. The undoped ZnO has the preferable orientation along the (002) direction, *i.e.* the films have the preferential orientation along *c*-axis. The doping of Mn^{2+} in Zn^{2+} lattice also prefers the *c*-axis orientation. But this addition of Mn^{2+} leads to the red shift the (002) plane. Whereas the addition of Mg^{2+} in Zn^{2+} lattice leads to red shift the (002) plane. In short, undoped and Mn doped ZnO prefers the absence of the secondary peaks. But in Mn and Mg doped ZnO, some of the new peaks are obtained. Hence simply the type of doping highly influences the preferable orientation. Fig. 1(b) confirms the presence of Mn and Mg for prepared thin films as a form of (002) plane shift. The characteristic diffraction peaks of pure and 'Mn' and 'Mg' doped ZnO thin films were well
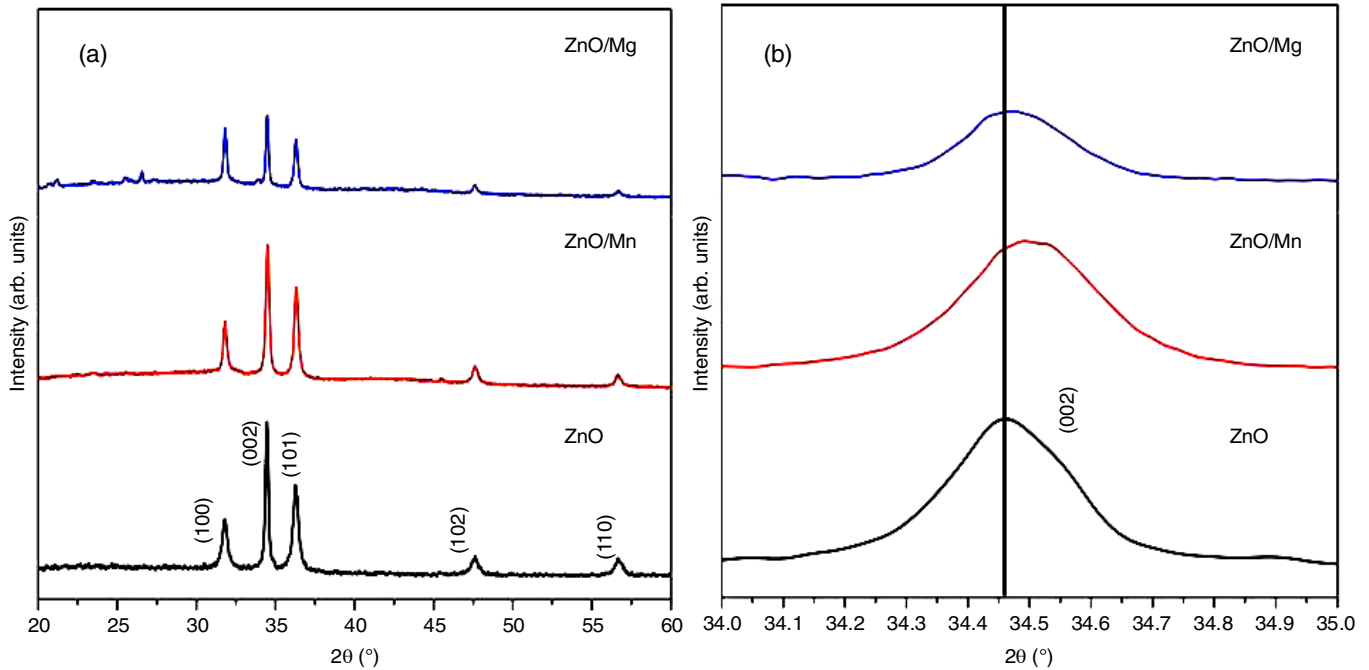
Fig. 1. XRD pattern of (Mn & Mg) doped ZnO thin films

matched with the standard diffraction JCPDS data card no: 36-1415. The peaks shows that the prepared ZnO are hexagonal structure with lattice parameter a = 3.249, c = 5.206. The crystalline peaks are having the good agreement with the standard JCPDS data. From the characterization peaks at $2\theta = 34.422$ confirm the presence of ZnO which is in the plane (002).

The structural parameters like crystallite size, dislocation density, strain, number of crystalline per unit area and lattice distortion were evaluated along with crystallite size using the formula. This parameter can be calculated using Scherer's formula from full width at half maximum (FWHM).

$$D = \frac{k\lambda}{\beta \cos\theta} \qquad (2)$$

where, constant 'k' is the shape factor = 0.94, 'λ' is wavelength of X-rays (1.5406 Å) 'θ' is the Bragg's angle and 'β' is FWHM. The grain size according to Debye-Scherrer's formula is maximum for undoped ZnO (~43 nm). When metal (Mn & Mg) is doped, the grain size of the films is decreased. This reduction of grain size due to the doping is maximum for Mg-doped ZnO rather than Mn-doped ZnO. The doping of Mg in Zn lattice leads to the decrease in very low grain size out of all the considered cases. The atmoic radii of Mn^{2+} and Mg^{2+} is 70 nm, where the atomic radii of Zn^{2+} is 74 nm. The calculated microstructural parameters are given in Table-1.

Dislocation density can be calculated from crystalline size (D) by the following equation:

$$\delta = \frac{1}{D^2} \qquad (3)$$

The strain (ε) and number of crystalline per unit area (N_C) were evaluated from the relations:

$$\varepsilon = \frac{\beta \cos\theta}{4} \qquad (4)$$

$$N_C = \frac{t}{D^3} \qquad (5)$$

The lattice distortion (LD) developed in thin films can be evaluated from the relation:

$$LD = \frac{\beta}{4\tan\theta} \qquad (6)$$

SEM and EDAX analysis: The surface morphology of the film is characterized by SEM analysis. Fig. 2a shows the pure ZnO thin film, which illustrate the formation of nano rods onto the surface. Fig. 2(b-c) shows the morphology of Mn and Mg doped ZnO thin films. It clearly illustrates the formation of sub-micrometer crystallites distributed more or less uniformly over the surface. Agglomeration of small crystallites also seems to be present in certain regions on the film surface. The film deposited at Mg doped has smooth and spindle like structure and uniformly covering the overall surfaces with good adherence [23,24]. The SEM image of Mn doped ZnO thin film shows the grains of spindle like shape without any cracks and pores.

This EDAX characterization confirms the presence of material coated on the film. Fig. 2d of EDAX results confirms the presence of zinc and oxygen in the prepared film. Fig. 2(e-f) shows the depends 'Mn' and 'Mg' were observed except that only the elemental carbon arises due to adhesion of carbon tape on the study used in the analysis. The results confirm the effective doping of 'Mn' and 'Mg' into ZnO thin film.

FTIR analysis: Presence of functional groups and its corresponding molecular vibrations were assessed from Fourier transform infrared spectroscopy. Fig. 3 represents the characteristic molecular vibrations of Mn and Mg doped and ZnO thin film in the range of 4000-400 cm^{-1}. The peak at 3434 cm^{-1} is due to O-H stretching vibration of surface absorbed water molecule. The absorption peak at 2926 cm^{-1} is due to the symmetric and asymmetric C-H bands. These shows the catalytic
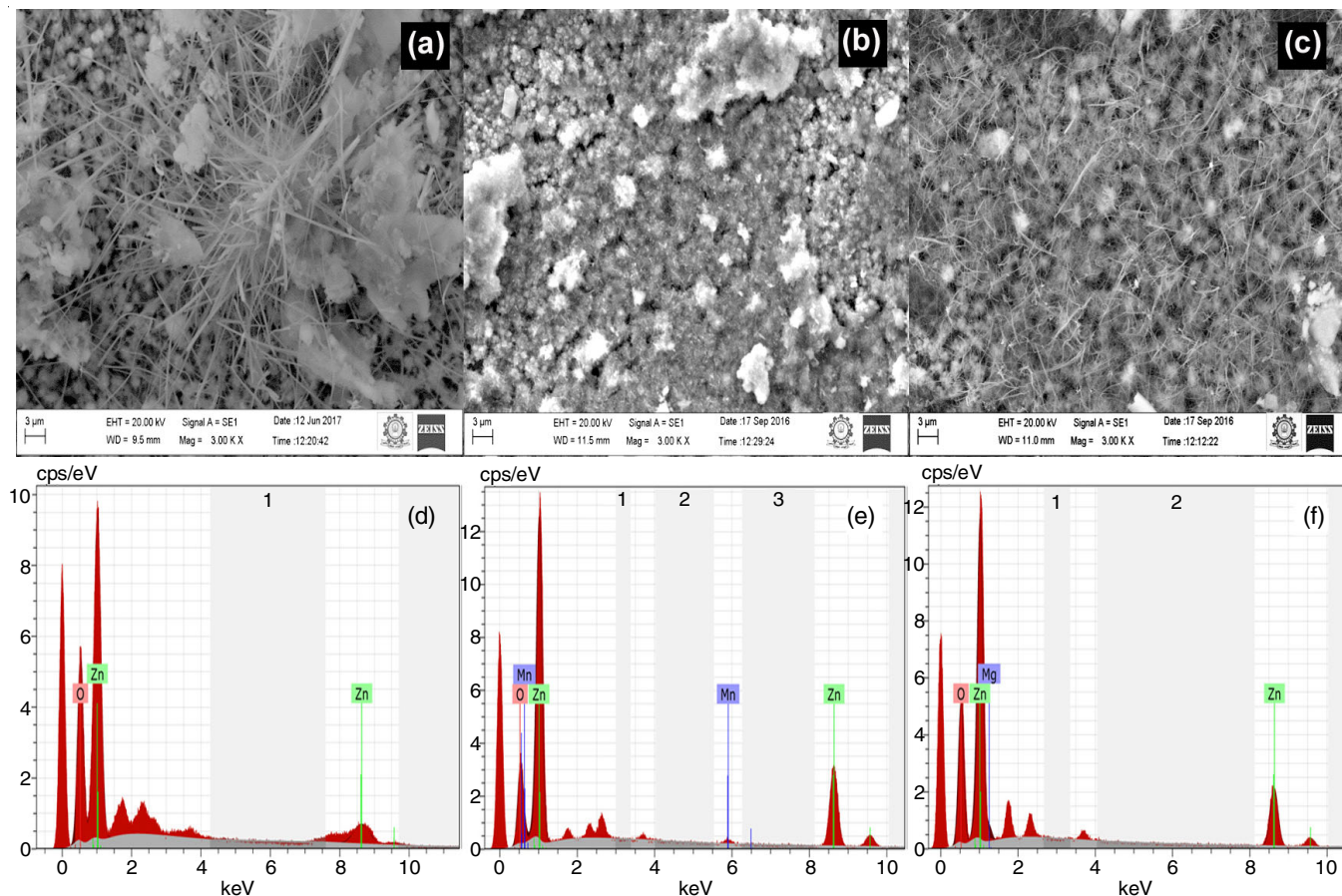
Fig. 2. (a-c) SEM images and (d-f) EDAX spectra of (Mn & Mg) doped ZnO thin films
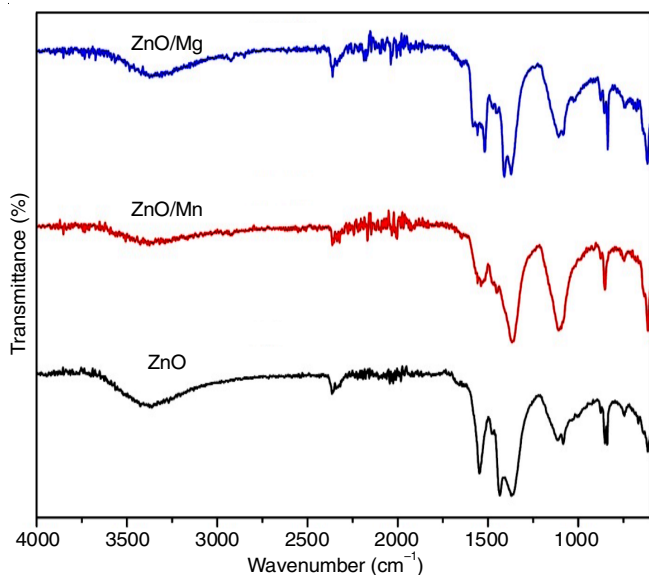
Fig. 3. FTIR spectra of (Mn & Mg) doped ZnO thin films

molecular vibration of Zn-O stretching. The recorded spectra for both the samples look alike and do not have any noticeable variation. This indicates that dopant atom Mn and Mg did not produce major physical changes in ZnO matrix.

UV-visible analysis: Figs. 4 and 5 depicted the optical absorbance and transmittance spectra of pure, Mn and Mg metal doped ZnO thin film. From the absorption spectrum, the pure one is having the maximum absorption compared with the Mn and Mg doped ZnO thin film. The absence of any other impurity peaks in both absorption and transmission spectra indicate the phase purity as well as no changes in ZnO lattice.

organic residues may presence along with the thin film sample. The peak at 2340 cm^{-1} is due to the existence of C-O stretching. The weak bands at 1614, 1398 and 1024 cm^{-1} are attributed to the symmetric and asymmetric C=O mode of zinc sulphate. The absorption peak at 874 cm^{-1} is a metal oxygen vibration frequency due to the changes in the micro-structural features by the addition of Mg^{2+} and Mn^{2+} ions into ZnO lattice. The sharp absorption peaks at 491 and 447 cm^{-1} is assigned to the

Fig. 4. Absorbance spectra of (Mn & Mg) doped ZnO thin films
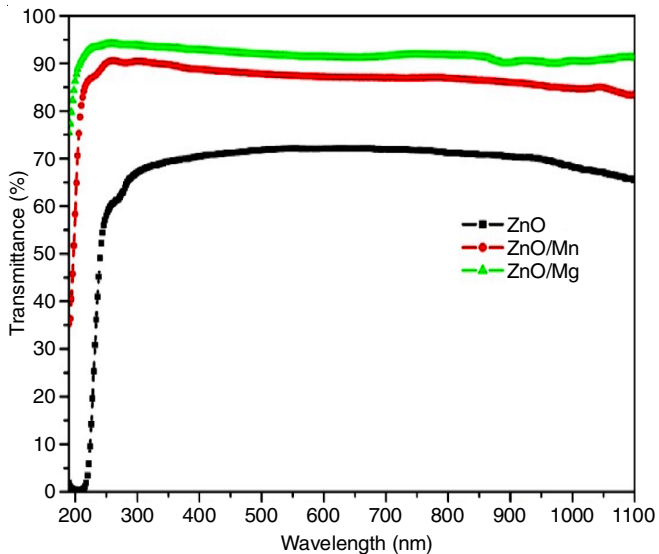
Fig. 5. Transmittance spectra of (Mn & Mg) doped ZnO thin films

Heavy doping may change the band gap or introduce new band levels in the host material. From the transmittance spectrum, Mg^{2+} doped ZnO is having the maximum transmittance compared with the other two materials (pure and Mn^{2+} ions doped ZnO).

Fig. 6 shows the variation of $(\alpha h\nu)^2$ with photon energy for various percentage of Mn & Mg doped ZnO thin film. The absorption coefficient (α) and incident photon energy ($h\nu$) can be related as:

$$\alpha = \frac{A(h\nu - E_g)^m}{h\nu}$$

where, A is a constant and E_g is the band gap of the material. The values of m depends upon the type of transition; which may have values 1/2, 2, and 3/2 corresponding to the allowed direct, allowed indirect and forbidden direct transitions respectively. From the above equation, it is clear that the plot of $(\alpha h\nu)^2$ versus $h\nu$, indicate a divergence of an energy value, E_g where the transition takes place. The values of optical band gap energies E_g were obtained by extrapolating the straight portion to $h\nu$ axis at $(\alpha h\nu) = 0$. In all the cases, the relation is linear in the absorbance region. It is due to the direct band-to-band transition. The obtained direct optical band gap values
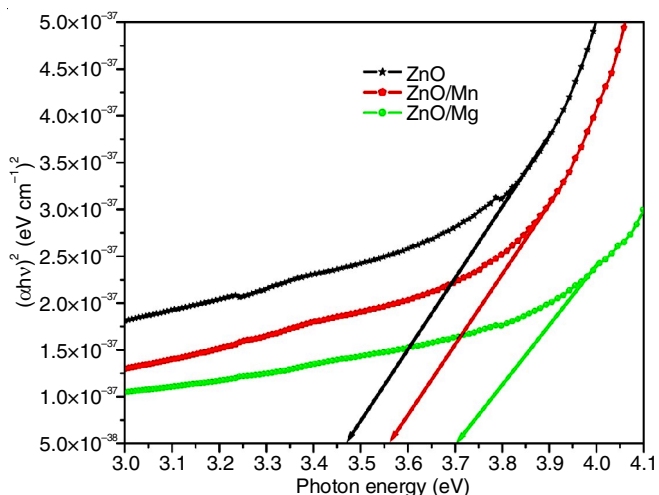
are 3.46, 3.56 and 3.7 eV for pure ZnO, Mn and Mg doped ZnO thin films, respectively.

Conclusion

Pure, Mn and Mg doped ZnO thin films were successfully coated on the glass substrate by using successive ionic layer adsorption and reaction (SILAR) method. The X-ray diffraction pattern confirms the hexagonal structure with primitive lattice and the characterization peak is matched with the JCPDS data (36-1415). The micro-structural parameter values are calculated from XRD data. The crystalline size of material was determined by Scherrer's formula range is 43-32 nm. The SEM image confirms the morphology of the particles and they are more or less uniformly in shape. The particle size of ZnO varies as indicated through SEM study. The EDAX spectra conforms the presence of Zn, O, Mn and Mg elements. The functional group in the coated film was investigated with FTIR and the characteristics vibrations of the different functional groups were identified. From the optical studies, high transmittance was achieved for all films. More than 95 % transmittance achieved for ZnO/Mg films. Minimum 65 % transmittance achieved for pure samples. The optical band gap values obtained in the range of 3.46-3.7 eV.

CONFLICT OF INTEREST

The authors declare that there is no conflict of interests regarding the publication of this article.

REFERENCES

1. A. Abdel-Galil, M.R. Balboul and A. Sharaf, *Physica B*, **477**, 20 (2015); https://doi.org/10.1016/j.physb.2015.08.001.
2. M.N.H. Mia, M.F. Pervez, M.K. Hossain, M. Reefaz Rahman, M.J. Uddin, M.A. Al Mashud, H.K. Ghosh and M. Hoq, *Results in Physics*, **7**, 2683 (2017); https://doi.org/10.1016/j.rinp.2017.07.047.
3. W.Y. Shim, K.A. Jeon, K.I. Lee, S.Y. Lee, M.H. Jung and W.Y. Lee, *J. Electron. Mater.*, **35**, 635 (2006); https://doi.org/10.1007/s11664-006-0112-2.
4. T. Srinivasulu, K. Saritha and K.T. Ramakrishna Reddy, *J. Modern Elect. Mater.*, **3**, 76 (2017); https://doi.org/10.1016/j.moem.2017.07.001.
5. K. Huang, Z. Tang, L. Zhang, J. Yu, J. Lv, X. Liu and F. Liu, *J. Appl. Surf. Sci.*, **258**, 3710 (2012); https://doi.org/10.1016/j.apsusc.2011.12.011.
6. S. Fujihara, C. Sasaki and T. Kimura, *J. Eur. Ceram. Soc.*, **21**, 2109 (2001); https://doi.org/10.1016/S0955-2219(01)00182-0.
7. Y.S. Wang, P.J. Thomas and P. O'Brien, *J. Phys. Chem. B*, **110**, 21412 (2006); https://doi.org/10.1021/jp0654415.
8. B.V. Rajendra, V. Bhat and D. Kekuda, *Adv. Mater. Res.*, **895**, 226 (2014); https://doi.org/10.4028/www.scientific.net/AMR.895.226.
9. M. Çavas, *J. Theoretical Appl. Phys.*, **11**, 325 (2017); https://doi.org/10.1007/s40094-018-0274-3.
10. K.K. Nagaraja, S. Pramodini, A. Santhosh Kumar, H.S. Nagaraja, P. Poornesh and D. Kekuda, *Opt. Mater.*, **35**, 431 (2013); https://doi.org/10.1016/j.optmat.2012.09.028.
11. S. Sharma, R.S. Kundu, A. Singh, S. Murugavel, R. Punia and N. Kishore, *Cogent Physics*, **2**, 1055623 (2015); https://doi.org/10.1080/23311940.2015.1055623.
12. R.K. Sharma, S. Patel and K.C. Pargaien, *Adv. Nat. Sci.: Nanosci. Nanotechnol.*, **3**, 035005 (2012); https://doi.org/10.1088/2043-6262/3/3/035005.
13. R. Mohan, S. Snega, K. Ravichandran and S. Vadivel, *J. Mater. Sci. Mater. Electron.*, **28**, 4414 (2017); https://doi.org/10.1007/s10854-016-6070-4.

Fig. 6. Tauc plots of (Mn & Mg) doped ZnO thin films

14. M. Rouchdi, E. Salmani, B. Fares, N. Hassanain and A. Mzerd, *Results in Physics*, **7**, 620 (2017);
https://doi.org/10.1016/j.rinp.2017.01.023.

15. L.R. Val'erio, N.C. Mamani, A.O. de Zevallos, A. Mesquita, M.I.B. Bernardi, A.C. Doriguetto and H.B. de Carvalho, *RSC Adv.*, **7**, 20611 (2017);
https://doi.org/10.1039/C7RA01200D.

16. M. Shatnawi, A.M. Alsmadi, I. Bsoul, B. Salameh, M. Mathai, G. Alnawashi, G.M. Alzoubi, F. Al-Dweri and M.S. Bawa'aneh, *Results in Physics*, **6**, 1064 (2016);
https://doi.org/10.1016/j.rinp.2016.11.041.

17. S. Yang and Y. Zhang, *J. Magn. Magn. Mater.*, **334**, 52 (2013);
https://doi.org/10.1016/j.jmmm.2013.01.026.

18. B.G. Shohany, L. Motevalizadeh and M.E. Abrishami, *J. Theoret. Appl. Phys.*, **12**, 219 (2018);
https://doi.org/10.1007/s40094-018-0302-3.

19. N. Tiwari, S. Kumar, A.K. Ghosh, S. Chatterjee, D. Bhattacharyya and S.N. Jha, *RSC Adv.*, **7**, 56662 (2017);
https://doi.org/10.1039/C7RA10748J.

20. M. Lorenz, R. Bottcher, S. Friedlander, A. Poppl, D. Spemann and M. Grundmann, *J. Mater. Chem. C Mater. Opt. Electron. Devices*, **2**, 4947 (2014);
https://doi.org/10.1039/c4tc00407h.

21. J.S. Fang, W.H. Luo, C.H. Hsu, J.C. Yang and T.K. Tsai, *J. Electron. Mater.*, **41**, 122 (2012);
https://doi.org/10.1007/s11664-011-1770-2.

22. S. Balamurali, R. Chandramohan, N. Suriyamurthy, P. Parameswaran, M. Karunakaran, V. Dhanasekaran and T. Mahalingam, *J. Mater. Sci. Mater. Electron.*, **24**, 1782 (2013);
https://doi.org/10.1007/s10854-012-1012-2.

23. S. Mondal, S.R. Bhattacharyya and P. Mitra, *J. Bull. Mater. Sci.*, **36**, 223 (2013);
https://doi.org/10.1007/s12034-013-0462-3.

24. M.A.R. Bonifácio, H.L. Lira, L.S. Neiva, R.H.G.A. Kiminami and L. Gama, *J. Mater. Res.*, **20**, 1044 (2017);
https://doi.org/10.1590/1980-5373-mr-2015-0765.